

# Acid-directed synthesis of SERS-active hierarchical assemblies of silver nanostructures†

Bin Zhang,<sup>a</sup> Ping Xu,<sup>\*ab</sup> Xinmiao Xie,<sup>a</sup> Hong Wei,<sup>c</sup> Zhipeng Li,<sup>c</sup> Nathan H. Mack,<sup>b</sup> Xijiang Han,<sup>a</sup> Hongxing Xu<sup>\*c</sup> and Hsing-Lin Wang<sup>\*b</sup>

Received 27th August 2010, Accepted 19th October 2010

DOI: 10.1039/c0jm02837a

SERS-active silver hierarchical assemblies are synthesized in solution by the assistance of small acid molecules. We here demonstrate the acid-directed self-assembly of metal nanoparticles (MNPs) into large systems with complex structures, without the application of any polymer surfactant or capping agent. It is verified that small acid molecules (citric acid, mandelic acid, *etc.*) incorporated into conventional solution chemistry can direct the assembly of MNPs into well-defined hierarchical structures. The constructed assembled structures with highly roughened surfaces can be highly sensitive SERS platforms, and the fabricated core-shell Ag wires show especially high SERS sensitivity toward the analyte melamine. The prepared Ag particles with hierarchical structures show no evident polarization-dependent SERS behavior, and this isotropic feature may be an advantage for highly sensitive SERS tags, since no certain incident polarization is required for molecule detection. We believe the subsequent addition of acid to induce formation of self-assembled structures can be a general synthetic platform to fabricate metal structures with complex morphologies.

## Introduction

The focus of nanoscience and nanotechnology is gradually shifting from the synthesis of individual components to their assembly into larger systems with well-defined structures.<sup>1–3</sup> Assemblies of nanoscaled metal building blocks with specific structures present collective optical, electronic, catalytic, and magnetic properties which are distinctly different from the corresponding individual nanoparticles.<sup>4–7</sup> Hierarchical self-assembly is the ultimate fabrication process for complex nanostructures and ensures molecular-level pattern precision and parallel processing.<sup>8–13</sup> A directed assembly of hierarchical CdS nanotube arrays from CdS nanoparticles shows enhanced solid-state electro-chemiluminescence,<sup>8</sup> and hierarchical assembly of multilayered hollow microspheres from an amphiphilic pharmaceutical molecule of azithromycin can be applied in controlled drug release, delivery and biocatalysis.<sup>9</sup> Metal ions are exploited to induce the formation of metal-cholate supramolecular helices, and it is interpreted that incorporation of metal ions may endow versatile functionalities and merits to the self-assembled nanohelices.<sup>12</sup> Complex structures formed by metal nanoparticle (MNP) assemblies have numerous cavities, interstitial sites, and void spaces that are known to generate enhanced electric field upon excitation that leads to surface-enhanced Raman scattering

(SERS).<sup>14–16</sup> However, for SERS applications, controlled synthesis of the so-called electromagnetic “hot spots” is difficult in most SERS-active materials as it requires exquisite preparation of MNPs with certain sizes and morphology and delicate manipulation of the nanoparticle assemblies.<sup>17–21</sup> Recent studies have shown an extremely strong local field enhancement in the gap between two closely spaced metal nanostructures.<sup>22–28</sup> Formation of such dimeric structures usually requires the use of organic and biological molecules to bridge two nanoparticles; however, the bridging molecules also prevent the target analyte from further being adsorbed onto the metal surface.<sup>29–35</sup> Furthermore, preparation of uniform and large-area SERS-active substrates consisting of metal nanoparticle dimers for commercial applications seems quite difficult. In solution chemistry for synthesizing MNPs, capping agents like poly(vinyl pyrrolidone) (PVP) and cetyltrimethyl ammonium bromide (CTAB) are commonly employed to induce anisotropic growth,<sup>36,37</sup> by which the size and morphology of the MNPs are successfully controlled. However, it is inevitable that a thin layer of polymer molecules will reside on the surface of the as-prepared MNPs even after repeated rinsing,<sup>38</sup> which may also disturb the adsorption of analyte molecules onto the metal surface or at least reduce the active surface area available for analyte binding.

Here we demonstrate for the first time the fabrication of novel self-assembled silver hierarchical structures simply by incorporating a small amount of acid in conventional solution chemistry, without the involvement of any polymer surfactant or capping agent. The assembly of silver nanoparticle (AgNP) components into well-defined complex structures under the direction of the incorporated acid has been confirmed by using different reducing agents. This acid-directed synthesis of metal structures precludes the sorption of polymer molecules on metal surfaces, and the obtained Ag particles have highly roughened morphology, which can be promising SERS substrates for sensing applications.

<sup>a</sup>Department of Chemistry, Harbin Institute of Technology, Harbin, 150001, China. E-mail: pxu@hit.edu.cn; Fax: +86 451 86418750; Tel: +86 451 86413702

<sup>b</sup>Physical Chemistry and Spectroscopy, Chemistry Division, Los Alamos National Laboratory, Los Alamos, NM, 87545, USA. E-mail: hwang@lanl.gov; Tel: +1 505 6679944

<sup>c</sup>Beijing National Laboratory for Condensed Matter Physics, Institute of Physics, Chinese Academy of Sciences, Beijing, 100190, China. E-mail: hongxingxu@aphy.iphy.ac.cn

† Electronic Supplementary Information (ESI) available: Additional SEM images and SERS spectra. See DOI: 10.1039/c0jm02837a/

## Experimental

### Materials

PANI emeraldine base (EB) (Aldrich), AgNO<sub>3</sub> (99.9999% Aldrich), mercaptobenzoic acid (MBA, Aldrich 90%), *N*-methyl-2-pyrrolidone (NMP, 99% Aldrich), malamine (99% Aldrich), heptamethylenimine (HPMI, 98% Acros), toluenesulfonic acid (98% Aldrich), mandelic acid (99% Aldrich), ascorbic acid (Aldrich) and citric acid (99.9% Fisher) were used as received.

### Preparation of Ag nanostructures using ascorbic acid as the reducing agent

1 ml AgNO<sub>3</sub> aqueous solution (1 M, 0.1 M, 0.05 M and 0.01 M) and 0.1 ml 0.25 M acid (citric acid, mandelic acid, or toluenesulfonic acid) were added to 10 mL deionized water in a 25 mL beaker with a magnetic stirrer in an ice–water bath.

An ascorbic acid aqueous solution (C<sub>6</sub>H<sub>8</sub>O<sub>6</sub>, 1 M) was then quickly injected into the vigorously stirred mixture. The added ascorbic acid was kept equimolar to that of silver ions. The solution became grey or khaki immediately in accordance with the added acid, and a large quantity of Ag particles were produced in a few minutes. After 15 min, the particles were collected by centrifugation and repeatedly rinsed with deionized water. Then the samples were dried in a vacuum drier at 60 °C. For comparison, preparation of Ag particles without the assistance of acid was also carried out.

### Preparation of core–shell Ag wires on polyaniline (PANI) films

(1) Preparation of PANI films. A typical procedure of fabricating the PANI film is described as follows: 4.14 g NMP, 0.747 g HPMI and 1.15 g PANI (EB) powder were mixed in a 12 ml Teflon vial. The mixture was stirred for 0.5–1 h to form a homogeneous solution, followed by being poured onto a glass substrate and spread into a wet film using a gardener's blade (Pompano Beach, FL) with a controlled thickness. The wet film was put in an oven at 50 °C for 12 h to evaporate the solvent and form a dense film. The dried film was kept in a water bath to let it peel off from the glass substrate. The resulting film was dried at room temperature, and then doped in 0.25 M citric acid aqueous solution for 2 days. (2) Growth of Ag nanowires on PANI films. The doped film was rinsed in deionized water to remove the surface adsorbed citric acid and cut into 5 mm × 5 mm pieces before nanowire growth. During the nanowire growth without adding the acid, the doped PANI films were immersed in 0.1 M AgNO<sub>3</sub> aqueous solution for different time periods to study the nanowire growth. The PANI films were then carefully rinsed with deionized water to terminate the nanowire growth and eliminate the residual salt, following by being dried in air at room temperature. (3) Fabrication of core–shell Ag structures on PANI films. The doped PANI films were firstly immersed in 0.1 M AgNO<sub>3</sub> aqueous solution for 10 s to initiate the nanowire growth. Then 10 μL 0.25 M citric acid or mandelic acid was added to the AgNO<sub>3</sub> aqueous solution to direct the assembly of Ag nanoparticles on the nanowires. For a mechanistic study of the core–shell Ag wire structure formation, samples were collected after citric acid was added for different time periods. The PANI films were then carefully rinsed with deionized water

to terminate the nanowire growth and eliminate the residual salt, following by being dried in air at room temperature.

### Characterization

Scanning electron microscopy (SEM) was carried out on a FEI Inspect F SEM to study the morphology and size of the Ag nanostructures. X-ray diffraction (XRD) measurements were carried out on a Shimadzu XRD-6000 diffractometer that uses fine line sealed Cu K $\alpha$  tube ( $\lambda = 1.5406 \text{ \AA}$ ) X-rays. The Ag particles were put in an MBA ethanol solution (1 mmol L<sup>-1</sup>) for 30 min and then rinsed by centrifugation with ethanol several times to remove the MBA residual on the surface. The MBA-adsorbed Ag particles were dispersed on glass substrates before the surface-enhanced Raman scattering (SERS) responses were determined. The core–shell Ag wires deposited on the substrate were immersed in melamine aqueous solutions of different concentrations for 30 min and then rinsed with deionized water to study the detecting sensitivity. The SERS spectra were recorded on a Kaiser Raman spectrometer through a 20 × (0.50 NA) microscope objective, coupled with a liquid-nitrogen-cooled charge-coupled device (CCD) detector (wavelength: 785 nm). The incident laser power was kept at 1 mW and total accumulation times of 10 s were employed. The Raman images were collected on a Renishaw in Via micro Raman spectroscopy system, using the TE air-cooled 576×400 CCD array in a confocal Raman system at the Raman shift of 1582 cm<sup>-1</sup> of the MBA molecule, while the laser light was blocked by a 633 nm edge filter. The objective used in the measurement is ×100 (NA = 0.95).

## Results and discussion

In a typical synthesis, a AgNO<sub>3</sub> aqueous solution (1 mL, 1 M) and an acid aqueous solution (0.1 mL, 0.25 M) were added to 10 mL deionized water in a 25 mL beaker with a magnetic stirrer in an ice–water bath. An ascorbic acid aqueous solution (C<sub>6</sub>H<sub>8</sub>O<sub>6</sub>, 1 mL, 1 M) was then quickly injected into the vigorously stirred mixture. The solution became grey or khaki immediately in accordance with the added acids, and a large quantity of Ag particles was produced in just a few minutes. It is interesting to find that the morphology of Ag assemblies is highly sensitive to the incorporated acid. Fig. 1 shows the SEM images of the Ag assemblies prepared with the assistance of different acids in low and high magnifications, which indicates that Ag particles with almost uniform structure corresponding to the incorporated acid can be produced by this acid-directed process. As shown in Fig. 1a, direct reduction of Ag<sup>+</sup> by ascorbic acid (no extra acid added) leads to irregular Ag particles with a size of about 1 μm. A magnified image indicates that these Ag particles are actually comprised of 50–100 nm thick Ag nanosheets (Fig. 1b), which resembles the structures obtained through a similar procedure.<sup>20</sup> However, addition of citric acid leads to the formation of perfect microspheres (~2 μm in diameter) that are assembled by numerous close packed 20 nm thick Ag nanosheets (Fig. 1c, d). The magnified image inset in Fig. 1c shows that these nanosheets, arranged along different directions, are actually formed by assembled nanoparticles. With mandelic acid, flower-like Ag particles are formed by loosely packed 50 nm

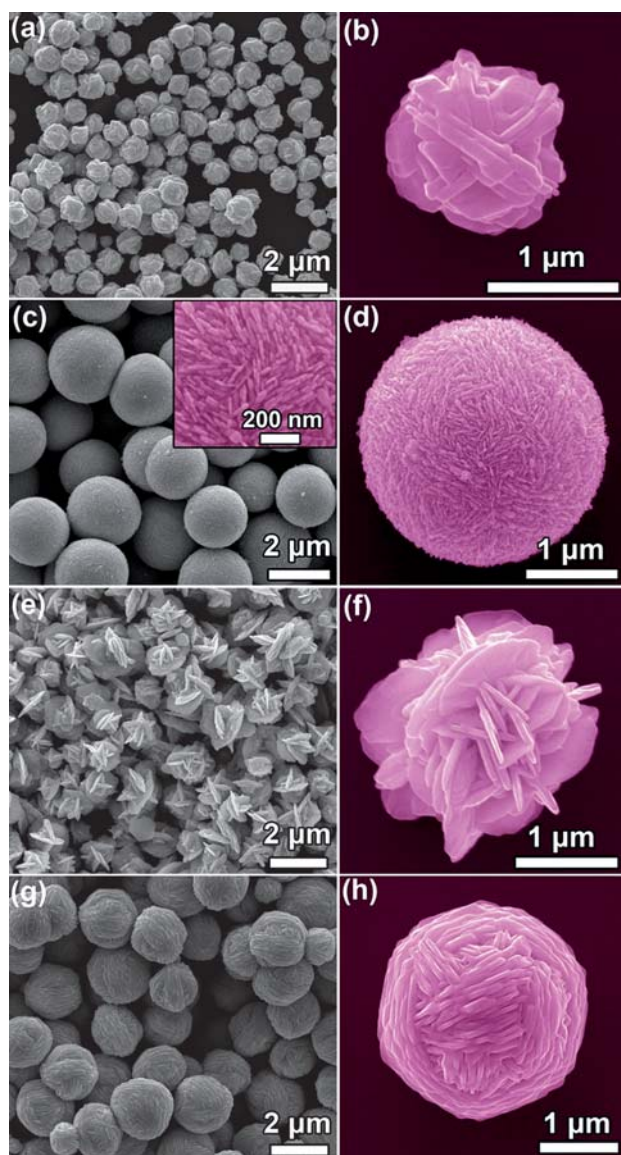


**Fig. 1** SEM images of Ag structures prepared through a chemical reduction of  $\text{Ag}^+$  ions ( $\text{AgNO}_3$ ) by ascorbic acid as the reducing agent, without using any polymer surfactant or capping agent. Before ascorbic acid was added to initiate the reduction reaction, (a, b) no acid, (c, d) citric acid, (e, f) mandelic acid, and (g, h) toluenesulfonic acid was added to the reaction system to control the assembly of the produced Ag nanostructures.

thick Ag nanosheets (Fig. 1e, f). One can find microscaled Ag yarn-balls assembled by cross-linked 50 nm thick Ag nanosheets in the presence of toluenesulfonic acid during the reaction (Fig. 1g, h).

The five peaks in the XRD patterns of the as-prepared Ag particles can be well indexed to the (111), (200), (220), (311), and (222) planes of the face-centered-cubic (fcc) Ag phase (Fig. 2), indicating that they are all well-crystallized. However, the appearance of all diffraction peaks and almost identical intensity ratios implies that the acid applied in the reaction system does not induce the anisotropic growth along a certain crystal plane, but just directs the nanoparticles to assemble into complex structures. It is clear that the acid added to complex the  $\text{Ag}^+$  ions

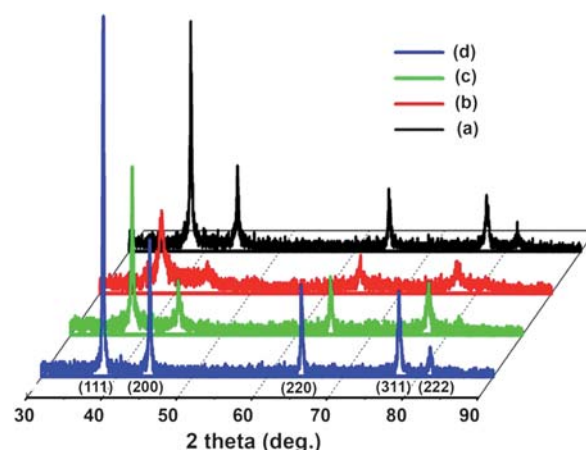


**Fig. 2** X-ray diffraction (XRD) patterns of the prepared hierarchical Ag particles with the assistance of (a) no acid, (b) citric acid, (c) mandelic acid, and (d) toluenesulfonic acid.

does not change the pristine Ag nanosheet formation when using ascorbic acid as the reducing agent, since all produced Ag particles are basically ensembles of Ag nanosheets. It has been revealed that the metal nanoparticle aggregates can be reversibly expanded and contracted by tuning the pH value of the solution system.<sup>39,40</sup> Here, the incorporated acid can greatly influence the structure and morphology of these nanosheet assemblies. To the best of our knowledge, this is the first evidence of directed assembly of MNPs into specific structures assisted only by small-molecule acids. Although the underpinning mechanism of the formation of Ag assemblies with different morphologies remains unclear, we believe that the acid molecules may complex with the  $\text{Ag}^+$  ions and/or be adsorbed on the Ag nucleates, which then direct the newly formed AgNPs in a way of assembly. By reducing the silver nitrate concentration, the grain size of the as-prepared Ag particles could be tuned from microns to several hundred nanometres, and the Ag nanosheet assemblies are getting more loosely packed (see Fig. S1 in ESI†). It is important to note that with a very low  $\text{AgNO}_3$  concentration (0.01 M), only unassembled AgNPs with an average size of 100–200 nm are visualized (see Fig. S2 in ESI†).

Assembled Ag structures prepared in the presence of various acids reveal strong SERS responses using mercaptobenzoic acid (MBA) as the probe molecule, and the detection sensitivity can easily reach ppm level, with an estimated enhancement factor of  $10^6$ – $10^7$  (see Fig. S3 in ESI†). It can be rationalized by the fact that the nanosheet assembly creates a nanoscale roughness over the particle surface, which will lead to amplification of the electromagnetic fields near the metal surface.<sup>14,20</sup> These hierarchical structures with different sizes may also be used as effective individual SERS-active tags in flow.<sup>41</sup> Incident polarization-dependent SERS of individual particles or wires has been of great interest recently, because Raman imaging can show the spatial distribution of SERS enhancement over the whole surface of a SERS tag, which renders a fundamental understanding of the SERS enhancement on a single particle.<sup>20,42</sup> Here we studied the SERS polarization properties of a single Ag particle using the Ag microsphere prepared by the assistance of citric acid (as shown in Fig. 1d). The Raman images were collected using the TE

air-cooled  $576 \times 400$  CCD array in a confocal Raman system at the Raman shift of  $1582 \text{ cm}^{-1}$  of the MBA molecule. Fig. 3a shows the polarization dependency for the particle as shown in Fig. 3b. One can see that the surface of the Ag microspheres can be a little modified after adsorbed with MBA molecules, as we also found on Ag nanosheets supported on polyaniline (PANI) membranes.<sup>43</sup> The Ag microspheres actually show very little polarization-dependent SERS enhancements over the surface, where almost identical SERS images are collected at different polarization angles (Fig. 3a). The polar plot in Fig. 3c shows that the SERS intensity of the whole particle does not present much polarization dependency. Other structures of the prepared Ag particles that have been investigated show very similar polarization-dependent SERS behavior. This isotropic feature may be an advantage for the prepared Ag hierarchical structures as highly sensitive SERS tags, since no certain incident polarization is required for molecule detection.

The acid-directed assembly of AgNPs into complex structures can be manifested in the growth of core-shell Ag wires using conducting PANI as the reducing agent. We have recently demonstrated the fabrication of metal nanostructures with various morphology and size through a direct chemical reduction by conducting polymers.<sup>43–50</sup> Here, on a citric acid doped PANI film, Ag nanowires (AgNWs) can grow on the surface in a matter of seconds. When the reaction period was extended to one hour, the PANI film would be fully covered with extremely long silver wires up to  $\sim 1 \text{ mm}$  that have polyhedral cross-sections (see Fig. S4 in ESI†). Interestingly, by adding a very small amount ( $10 \mu\text{L}$ ,  $0.25 \text{ M}$ ) of citric acid after the AgNW growth was initiated ( $10 \text{ s}$  later), we found that the added acid could direct the subsequent AgNPs assembly into nanosheets on the nanowire surfaces (Fig. 4), a result that agrees well with our

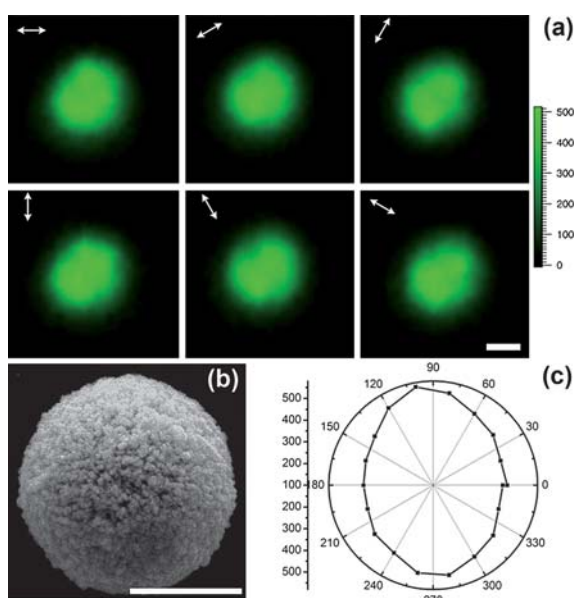


**Fig. 3** (a) The Raman images of a single Ag microsphere under different incident polarizations. The arrows show the different polarizations. (b) The corresponding SEM image of the Ag microsphere for SERS polarization study. (c) Polar plot of the strongest Raman intensities read from the SERS images. Scale bar:  $1 \mu\text{m}$ .

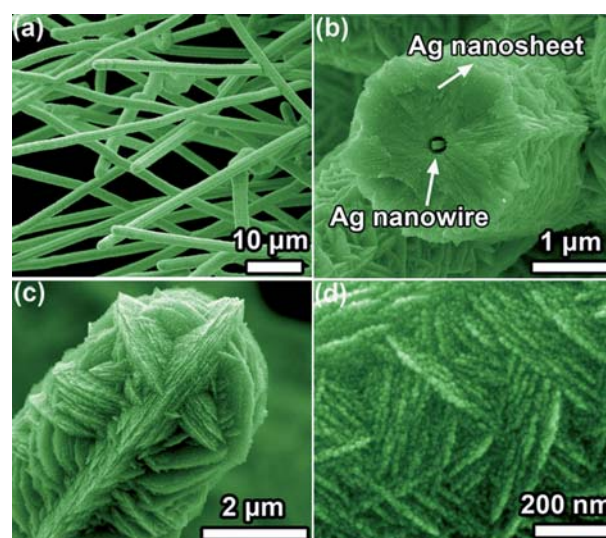


**Fig. 4** (a) Low-magnification SEM image of the produced Ag wires, and magnified SEM images of (b) the cross-section of a typical core-shell Ag wire, (c) the tip of a core-shell Ag wire covered by nanosheet assemblies, and (d) the surface of a wire showing that the nanosheets are actually assembled by nanoparticles.

finding that citric acid that adsorbs on the MNPs would induce the MNPs to assemble into sheet-like structures.<sup>43</sup> Fig. 4a shows the Ag wires grown on a PANI film after extra citric acid was added for 1 h, which reveals that lateral growth of the assembled nanosheets on top of the nanowire after addition of citric acid would cause concomitant inhibition of the radial growth of nanowires, leading to wires with limited aspect ratios. Fig. 4b presents a core-shell structure consisting of AgNW ( $100\text{--}200 \text{ nm}$  in diameter) as the core and assembled nanosheets as the shell, with a shell thickness of about  $1 \mu\text{m}$ . The top surface in Fig. 4c clearly shows that the end of the wire is capped by the nanosheet assemblies, which is believed to terminate the radial growth of the AgNWs, leading to much shorter wires than those prepared without the extra addition of citric acid (see Fig. S4 in ESI†). From Fig. 4d, one can see the interlaced Ag nanosheets are assembled by AgNPs with a mean size of about  $40 \text{ nm}$  and each nanosheet is actually formed by one single layer of AgNP assemblies, but not common smooth nanosheets as prepared from solution chemistry.<sup>18</sup> This result verifies that the wire structure is formed by the assembly of nanosheets on the surfaces of the original AgNWs.

As shown in Fig. 5, the XRD pattern of the prepared core-shell Ag wires differs a lot from those of the Ag particles with hierarchical structures as found in Fig. 2, which indicates a dominant diffraction peak corresponding to the (111) plane of fcc Ag phase. One can only see very limited diffractions from (200), (220), (311), and (222) planes. As found in most single crystalline AgNWs, (111) plane would be the preferable growth direction when a proper surfactant or capping agent was applied during the controlled anisotropic growth.<sup>51,52</sup> Here, when citric acid was introduced to induce the assembly of AgNPs onto the pre-existing AgNWs on the PANI films, the AgNPs would also grow with an anisotropic feature along the [111] crystal plane. As a result, a dominant (111) diffraction peak was observed in the XRD pattern of the core-shell Ag wires.

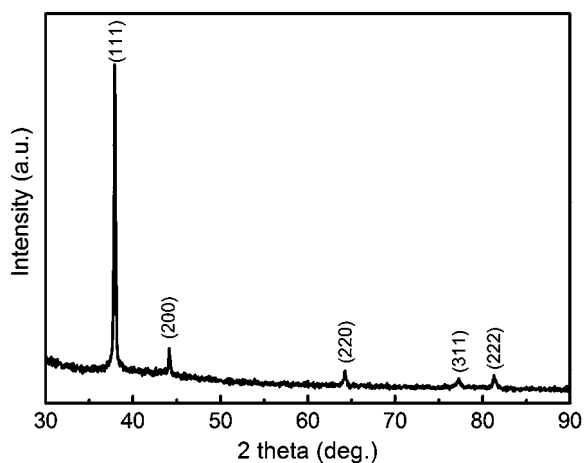


Fig. 5 XRD pattern of the prepared core-shell Ag wires.

The acid-directed nanosheet growth and assembly on the AgNWs can be further validated by a time-dependent SEM study of the structure evolution of the core-shell Ag wires (Fig. 6). Growth of AgNWs on PANI films is a very quick process, smooth AgNWs with diameters of about 200 nm can be seen only after 10 s (Fig. 6a). Immediately after citric acid was added in the AgNO<sub>3</sub> solution, an initial aggregation of newly formed AgNPs on the surface of AgNWs can be distinguished (Fig. 6b), which again verifies that the incorporated acid directs the newly formed AgNPs in a way of assembly. It is interesting to find that instead of size growth, the AgNPs assemble in the form of nanosheets in an extended period (Fig. 6c). Further growth leads to well-defined interlaced structures, as well as increased diameters of the Ag wire structures (Fig. 6d, e). After one hour, core-shell Ag wires with an average diameter of about 2 μm can be found, with the shells consisting of nanosheets that are formed by assembled AgNPs (Fig. 6f). By using same amount of mandelic acid instead of citric acid, we also get assembled nanosheet structures that are loosely packed on the wires (see Fig. S5 in ESI<sup>†</sup>), similar to the case of Ag particles. We believe that this subsequent addition of citric acid to induce formation of core-shell structures can be

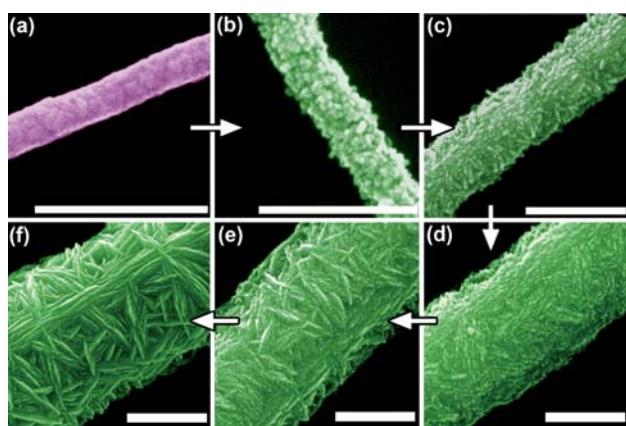


Fig. 6 Time-dependent SEM images of citric acid directed formation of a core-shell Ag wire: (a) nanowire growth on PANI film for 10 s, (b)–(f): after citric acid was added for 10 s, 1 min, 5 min, 10 min and 60 min, respectively. Scale bar: 1 μm.

a general synthetic platform to fabricate metal structures with complex morphologies.

We find this core-shell Ag structure shows especially strong SERS response for the detection of melamine—a milk contaminant added to artificially inflate the reading of protein level and causes acute kidney failure, with several fatalities. As shown in Fig. 7, the most intense peak in the SERS spectrum of melamine observed at 679 cm<sup>-1</sup> is assigned to the ring breathing mode II and involves in-plane deformation of the triazine ring in melamine molecules, and a barely visible peak around 984 cm<sup>-1</sup> arises from the ring breathing mode I of the triazine ring.<sup>53,54</sup> It can be seen that the sensitivity of detecting melamine on these core-shell Ag wires reaches 5 ppm, almost one of the highest sensitivities ever reported and is very promising for fast detection of additives in dairy products.<sup>54</sup> The interlaced nanosheets create abundant interstitial sites, which can be “hot spots” in SERS measurement. Moreover, the AgNPs that form the nanosheets may facilitate analyte molecule binding and gaps between two AgNPs can present similar SERS enhancement as found in metal dimers.<sup>14,55,56</sup> The intensity change of the Raman peak at 679 cm<sup>-1</sup> with the melamine concentration is shown in the inset of Fig. 7. When the concentration is 5 ppm, the peak intensity is about 3500. When the concentration is increased to 10 ppm, the peak intensity is increased to about 10 000. That is to say, when the number of molecules became double, the SERS intensity became more than double. Considering the experimental uncertainty, it can be concluded that when the concentration is not higher than 10 ppm, all melamine molecules adsorbed on the core-shell Ag structures are enhanced adequately, because there are enough “hot spots” for those molecules. When the concentration is increased further to 50 ppm, the Raman intensity of the 679 cm<sup>-1</sup> peak is increased to about 22 000, which is only about double the intensity of the 10 ppm case. The decrease of the enhancement for the samples of high concentration should be caused by the crowd of the molecules compared with the “hot

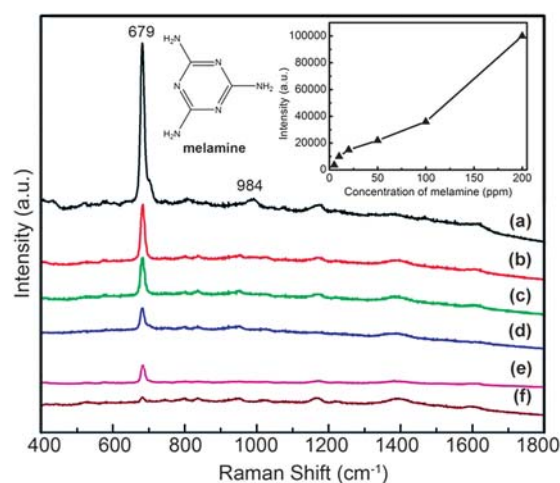


Fig. 7 SERS spectra of melamine in different concentrations taken on core-shell Ag wire structures: (a) 200 ppm, (b) 100 ppm, (c) 50 ppm, (d) 20 ppm, (e) 10 ppm, and (f) 5 ppm. Measurements were conducted with a 10 s exposure and 1 mW laser power. Inset shows the relationship between Raman intensity of the 679 cm<sup>-1</sup> band and concentration of melamine solution.

spots". When a large amount of molecules are adsorbed on the Ag structures, some molecules may locate at the spots which are not so hot, therefore, the averaged enhancement factor will be decreased. Actually, when the concentration is high, the melamine will crystallize on the Ag wires, and the normal Raman scattering will contribute to the detected Raman signal. An SEM image of the Ag wires after immersing in melamine solution of 100 ppm shows that the melamine can evenly crystallize on these wires (see Fig. S6 in ESI†).

## Conclusions

In summary, without the assistance of any surfactant or capping agent, small acid molecules can be applied to direct the assembly of MNPs into well-defined hierarchical structures. This synthesis technique of metal structures precludes the sorption of polymer molecules on metal surfaces. The acid-directed assembly of MNPs has been confirmed by using both ascorbic acid and polyaniline as the reducing agents. The as-prepared self-assembled structures with highly roughened surfaces can be highly sensitive SERS platforms for the detection of chemical or biological molecules. The Ag particles with hierarchical structures show no polarization dependency of the incident laser, and this feature can be an advantage for molecule detection since no certain incident polarization is required during SERS measurement. Notably, the fabricated core-shell Ag wires show especially high SERS activity toward melamine, with a detection sensitivity of 5 ppm. We believe this facile acid-directed fabrication of MNPs into larger systems with hierarchical structures may open up a new avenue for fabricating complex assembled architectures and exploring emerging properties that have been previously inaccessible.

## Acknowledgements

HLW acknowledges the financial support from Laboratory Directed Research and Development (LDRD) fund under the auspices of DOE, BES Office of Science, and the National Nanotechnology Enterprise Development Center (NNEDC). This work was performed in part at the U.S. Department of Energy, Center for Integrated Nanotechnologies, at Los Alamos National Laboratory (Contract DE-AC52-06NA25396) and Sandia National Laboratories (Contract DE-AC04-94AL85000). PX thanks the support from the Joint Educational Ph.D. Program of Chinese Scholarship Council (CSC), NSFC (No. 20776032, 21071037) and Special Fund of Harbin Technological Innovation (2010RFXXG012). HXX thanks the financial support from NSFC (No. 10625418, 10874233) and MOST (No. 2007CB936800, 2009CB930700).

## Notes and references

- R. Klajn, K. J. M. Bishop, M. Fialkowski, M. Paszewski, C. J. Campbell, T. P. Gray and B. A. Grzybowski, *Science*, 2007, **316**, 261.
- R. Bardhan, O. Neumann, N. Mirin, H. Wang and N. J. Halas, *ACS Nano*, 2009, **3**, 266.
- K. J. M. Bishop, C. E. Wilmer, S. Soh and B. A. Grzybowski, *Small*, 2009, **5**, 1600.
- V. Polshettiwar, B. Baruwati and R. S. Varma, *ACS Nano*, 2009, **3**, 728.
- M. Rycenga, J. M. McLellan and Y. Xia, *Adv. Mater.*, 2008, **20**, 2416.
- Didiot, S. Pons, B. Kierren, Y. Fagot-Revurat and D. Malterre, *Nat. Nanotechnol.*, 2007, **2**, 617.
- F. X. Redl, K. S. Cho, C. B. Murray and S. O'Brien, *Nature*, 2003, **423**, 968.
- C. Wang, Y. E. L. Fan, Z. Wang, H. Liu, Y. Li, S. Yang and Y. Li, *Adv. Mater.*, 2007, **19**, 3677.
- H. Zhao, J.-F. Chen, Y. Zhao, L. Jiang, J.-W. Sun and J. Yun, *Adv. Mater.*, 2008, **20**, 3682.
- L. Piot, C. Marie, X. Feng, K. Müllen and D. Fichou, *Adv. Mater.*, 2008, **20**, 3854.
- C. Li, A. D. Schlüter, A. Zhang and R. Mezzenga, *Adv. Mater.*, 2008, **20**, 4530.
- Y. Qiao, Y. Lin, Y. Wang, Z. Yang, J. Liu, J. Zhou, Y. Yan and J. Huang, *Nano Lett.*, 2009, **9**, 4500.
- F. Tancini, D. Genovese, M. Montalti, L. Cristofolini, L. Nasi, L. Prodi and E. Dalcanale, *J. Am. Chem. Soc.*, 2010, **132**, 4781.
- H. Xu, E. J. Bjerneld, M. Käll and L. Börjesson, *Phys. Rev. Lett.*, 1999, **83**, 4357.
- H. Xu, J. Aizpurua, M. Käll and P. Apell, *Phys. Rev. E: Stat. Phys., Plasmas, Fluids, Relat. Interdiscip. Top.*, 2000, **62**, 4318.
- Y. Fang, N.-H. Seong and D. D. Dlott, *Science*, 2008, **321**, 388.
- E. Katz and I. Willner, *Angew. Chem., Int. Ed.*, 2004, **43**, 6042.
- A. Courty, A.-I. Henry, N. Goubet and M.-P. Pileni, *Nat. Mater.*, 2007, **6**, 900.
- M. Linh Tran, S. P. Centeno, J. A. Hutchison, H. Engelkamp, D. Liang, G. Van Tendeloo, B. F. Sels, J. Hofkens and H. Uji-i, *J. Am. Chem. Soc.*, 2008, **130**, 17240.
- H. Liang, Z. Li, W. Wang, Y. Wu and H. Xu, *Adv. Mater.*, 2009, **21**, 4614.
- H. Wei, A. Reyes-Coronado, P. Nordlander, J. Aizpurua and H. Xu, *ACS Nano*, 2009, **4**, 2649.
- Y. Sawai, B. Takimoto, H. Nabika, K. Ajito and K. Murakoshi, *J. Am. Chem. Soc.*, 2007, **129**, 1658.
- M. Ringler, T. A. Klar, A. Schwemer, A. S. Susa, J. Stehr, G. Raschke, S. Funk, M. Borowski, A. Nichtl, K. Kürzinger, R. T. Phillips and J. Feldmann, *Nano Lett.*, 2007, **7**, 2753.
- J. P. Camden, J. A. Dieringer, Y. Wang, D. J. Masiello, L. D. Marks, G. C. Schatz and R. P. Van Duyne, *J. Am. Chem. Soc.*, 2008, **130**, 12616.
- P. H. C. Camargo, M. Rycenga, L. Au and Y. Xia, *Angew. Chem., Int. Ed.*, 2009, **48**, 2180.
- W. Li, P. H. C. Camargo, X. Lu and Y. Xia, *Nano Lett.*, 2009, **9**, 485.
- H. Wei, F. Hao, Y. Huang, W. Wang, P. Nordlander and H. Xu, *Nano Lett.*, 2008, **8**, 2497.
- H. Wei, U. Håkanson, Z. Yang, F. Höök and H. Xu, *Small*, 2008, **4**, 1296.
- C. A. Mirkin, R. L. Letsinger, R. C. Mucic and J. J. Storhoff, *Nature*, 1996, **382**, 607.
- A. P. Alivisatos, K. P. Johnsson, X. G. Peng, T. E. Wilson, C. J. Loweth, M. P. Bruchez and P. G. Schultz, *Nature*, 1996, **382**, 609.
- C. J. Loweth, W. B. Caldwell, X. G. Peng, A. P. Alivisatos and P. G. Schultz, *Angew. Chem., Int. Ed.*, 1999, **38**, 1808.
- J. P. Novak and D. L. Feldheim, *J. Am. Chem. Soc.*, 2000, **122**, 3979.
- R. Sardar, T. B. Heap and J. S. Shumaker-Parry, *J. Am. Chem. Soc.*, 2007, **129**, 5356.
- S. Y. Park, A. K. R. Lytton-Jean, B. Lee, S. Weigand, G. C. Schatz and C. A. Mirkin, *Nature*, 2008, **451**, 553.
- X. Wang, G. Li, T. Chen, M. Yang, Z. Zhang, T. Wu and H. Chen, *Nano Lett.*, 2008, **8**, 2643.
- Y. Sun and Y. Xia, *Science*, 2002, **298**, 2176.
- H.-L. Wu, C.-H. Chen and M. H. Huang, *Chem. Mater.*, 2009, **21**, 110.
- I. Száraz and W. Forsling, *Langmuir*, 2001, **17**, 3987.
- Y. Chen and C. Mao, *Small*, 2008, **4**, 2191.
- X. Han, Y. Li, S. Wu and Z. Deng, *Small*, 2008, **4**, 326.
- G. Goddard, L. O. Brown, R. Habberset, C. I. Brady, J. C. Martin, S. W. Graves, J. P. Freyer and S. K. Doorn, *J. Am. Chem. Soc.*, 2010, **132**, 6081.
- S. J. Lee, J. M. Baik and M. Moskovits, *Nano Lett.*, 2008, **8**, 3244.
- P. Xu, N. H. Mack, S. Jeon, S. K. Doorn, X. Han and H.-L. Wang, *Langmuir*, 2010, **26**, 8882.
- H.-L. Wang, W. Li, Q. X. Jia and E. Akhadorov, *Chem. Mater.*, 2007, **19**, 520.

- 45 Y. Gao, C.-A. Chen, H.-M. Gau, J. A. Bailey, E. Akhadov, D. Williams and H.-L. Wang, *Chem. Mater.*, 2008, **20**, 2839.
- 46 P. Xu, X. Han, C. Wang, B. Zhang, X. Wang and H.-L. Wang, *Macromol. Rapid Commun.*, 2008, **29**, 1392.
- 47 P. Xu, X. Han, B. Zhang, N. H. Mack, S. Jeon and H.-L. Wang, *Polymer*, 2009, **50**, 2624.
- 48 H.-H. Shih, D. Williams, N. H. Mack and H.-L. Wang, *Macromolecules*, 2009, **42**, 14.
- 49 P. Xu, S.-H. Jeon, N. H. Mack, S. K. Doorn, D. J. Williams, X. Han and H.-L. Wang, *Nanoscale*, 2010, **2**, 1436.
- 50 P. Xu, B. Zhang, N. H. Mack, S. K. Doorn, X. Han and H.-L. Wang, *J. Mater. Chem.*, 2010, **20**, 7222.
- 51 A. Bid, A. Bora and A. K. Raychaudhuri, *Phys. Rev. B: Condens. Matter Mater. Phys.*, 2006, **74**, 035426.
- 52 Y. Sun, B. Gates, B. Mayers and Y. Xia, *Nano Lett.*, 2002, **2**, 165.
- 53 M. Lin, L. He, J. Awika, L. Yang, D. R. Ledoux, H. Li and A. Mustapha, *J. Food Sci.*, 2008, **73**, T129.
- 54 L. He, Y. Liu, M. Lin, J. Awika, D. R. Ledoux, H. Li and A. Mustapha, *Sens. Instrum. Food Qual. Saf.*, 2008, **2**, 66.
- 55 H. Xu and M. Käll, *ChemPhysChem*, 2003, **4**, 1001.
- 56 T. Shegai, Z. Li, T. Dadosh, Z. Zhang, H. Xu and G. Haran, *Proc. Natl. Acad. Sci. U. S. A.*, 2008, **105**, 16448.